New Tube-Based Shooting and Bouncing Ray Tracing method

Chiya Saeidi, Farrokh Hodjatkashani
dept. of Electrical Engineering
Iran University of Science and Technology
Tehran, Iran
csaeidi@ee.iust.ac.ir, kashani@iust.ac.ir

Azim Fard
Communications Regularity Authority
Tehran, Iran
Azimfard@cra.ir

Abstract— **In this paper, a new shooting and bouncing (SBR) ray-tracing method is presented for wave propagation simulating, based on the tube shooting. Two concepts of center-ray tube and lateral-ray tube are defined and then compared in different aspects of accuracy and computational time wherein the use of lateral-ray tube revealed as important step forward in ray tracing accuracy but more time consuming. An acceleration technique developed based on ray tubes coherency that deals with ray-sharing characteristic of tube. New concept of two-ray tube tracing (TRTT) benefiting four-ray tube configuration is presented. A computational procedure developed to implement TRTT technique for simulation of wave propagating through large complex three-dimensional (3D) objects. To verify accuracy of presented TRTT technique and relevant computational procedure, a simple 4 buildings scenario analyzed using CST MICROWAVE STUDIO®. Moreover, field measurement values and TRTT simulation results compared in an urban environment on 910 MHz. The good agreement between simulation results and the measurements validates presented technique. Consequently, proposed technique provides an efficient ray tracing method while retains same accuracy as for four-ray tube launching. Moreover, this method can be used for evaluation of wireless channel characteristics by providing enough 3D information of tube configuration for 3D analysis of environments.**

Keywords- Ray tracing method; radio propagation.

I. INTRODUCTION

Recently, the concept of using site-specific knowledge of the physical environment to fairly predict the radio propagation draws a great amount of researcher's attention. Site-specific models are based on numerical methods such as the ray-tracing method and FDTD method. Ray-tracing models, utilizes physical environmental data to provide large-scale path loss information and small-scale multipath fading characteristics. Hence ray-tracing modeling is the most promising and widely used technique for radio wave propagation prediction. There are two ray tracing methods: one is called the "image" method (or inverse method), and the other is the "brute force" method (or direct method). The fundamental process of a direct ray tracing method is the SBR algorithm [1]. In this paper we focus on the ray launching and tracing issues under SBR algorithm. Launched ray is either treated as a ray tube [4] or a ray cone [2]–[5]. Ray cones have to overlap when used to cover the spherical wavefront at the transmitting location. For the cone scheme, the reception test can be easily carried out by using a reception sphere centered at the receiving point with radius as a function of the angle between two adjacent rays and the total length of the ray [2]. Since ray cones are overlapped, when a receiving point is located in the overlapping area between the ray cones, the receiver will consider received rays twice [6]. In the case of using ray tubes, the spherical wavefront can be covered without overlapping rays. There are various ways to subdivide the sphere surface into equal area "patches" that are all the similar shape and completely cover the surface without gaps. Regular triangles, squares, and hexagons can completely cover an area with equal size and shape objects without leaving gaps. Tube creating can be categorized into two different schemes using center-ray tubes (a ray is shot from the center of the patch wavefront) or lateral-ray tubes (rays are shot from vertices of the patch wavefront), depending on the number of rays chosen to build a tube. Although all above subdividing ways create rays with nearly constant separation (because of considering their spreading factor), but the reception sphere overlapping problem would happen in the center-ray tube scheme. Double counting shortcoming, which consumes time and memory, should be eliminated in post processing of raw output. Moreover, because there is only one ray representing a spreading tube, some errors could be occurred in detecting and localizing obstructions. Also, an inaccurate and expensive edge-obstruction test has to be employed, once a tube hit an object, especially in 3D scenarios. Moreover, the computation of the field transported by each one of the ray tubes generated in the diffraction is very cumbersome, because the diffracted field is not a spherical wave, as is usually assumed in center-ray tracing algorithm [11]. Using lateral-ray tube tracing methods, even though, can be a remedy of many drawbacks of center-ray method, but the cost of casting lateral rays instead of a center ray is multiplied by the number of rays per tube.

This paper presents a new tube tracing method using quadrilateral patch as wavefront of tube –four lateral-ray– to develop an accurate tracing procedure while keeping the computation cost only two times of those for center-ray tube tracing. Using this method makes it possible to detect all important obstacles without edge-obstruction testing, even in large 3D scenarios including complicated shapes. In Section II, different aspects of center-ray and lateral-ray methods compared. The new method presented through Sections III and IV. Section V provides an example for implementation of the

method. Finally, Sections VI and VII demonstrate achieved results and good agreement of TRTT with MoM and measurement.

II. CENTER-RAY VS. LATERAL-RAY TUBE TRACING

To keep all ray manipulation routines general, it is desirable that each ray tube occupy the same solid angle and each wavefront to have an identical shape and size at a distance r from the transmitter. Regular triangles, squares, and hexagons can completely cover an area with equal size and shape objects without leaving gaps. Although these subdividing ways suggest a constant angular separation of the rays, but shooting a ray from the center of tube segment representing related tube (center-ray tracing), leads several shortcomings as indicated below. In order to check if a ray is received, in the case of center-ray tube tracing, the intersection test of reception sphere need to be done. It is notable that the use of a reception sphere requires that the rays must be launched such that each ray is separated from neighboring rays by a nearly constant angle. So, if nearly uniform separation is not maintained, the test ray will not be separated from adjacent rays by similar angles and the reception sphere would lose its physical significance [2]. Basically, application of center-ray tubes without considering their lateral geometry demands to employ concept of reception sphere at the receiving point which in turn means overlapping of received adjacent ray tubes, consequently (Fig. 1a).

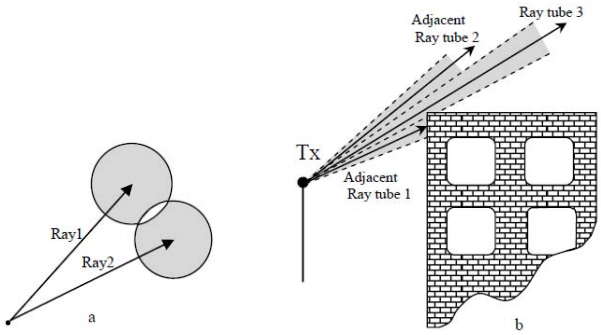

Figure 1. a) overlapping of received adjacent ray tubes and b) tubes missing objects in center-ray tube tracing (tube 3)

Therefore, mentioned overlapping causes double counting shortcoming and should be eliminated in a time and memory consuming post processing of raw output. In [6], a method of distributed wavefronts was developed to remedy this problem. This method improves the accuracy of the calculated fields but is relatively complex to realize and is inherently inaccurate. In [7] an accurate approach proposed, based on characterizing received rays according to the objects they encounter from the source to the reception point. Compared to the previous remedies, even though, it is simple and effective but at any reception point storing of a sequence of mechanisms and a cumbersome analysis of receiving rays is necessary.

In center-ray tube tracing, tubes could intersect objects physically without detection numerically during propagation, and in this circumstance, tubes miss those objects in the environment. Fig 4b illustrates the above drawback of center-ray method as a common case when the radio waves propagate close to rooftops. This Figure, additionally, depicts how a missed obstacle could lead to fail predicting field in a shadow. Employing of lateral ray tube diminishes the problem and no significant object near to the source would be left unconsidered. However, missing some objects can never be cured that way. The similar problem for lateral-ray tubes may happen. Wherever, the object dimension is inside the ray tube, when the obstacle is small or it is placed in far distance despite of its big dimension. For a tube with sufficient small angular separation of its rays (e.g. one degree), a small missed object would have only insignificant local contribution. From the other hand, strength of arrived rays to the far big missed obstacle satisfactorily attenuated, thus, cannot cause a considerable change in result.

The complexity in processing of edge obstruction test in 3D cases is another weakness of center-ray method. To find out diffraction occurrence, the edges of the walls serve as a line of receiving points and need to be examined whether a ray hits the corresponding finite cylinder of reception sphere radii.

III. TUBE BELT GEOMETERY

In lateral-ray tube methods [4][5], as explained in section II, any initial ray tube has to be traced to find its contribution in receiving point while in new approach a belt of tubes sharing two-rays is traced and analyzed simultaneously. So, the cost of procedure could be half in computation time and memory point of view. The radiated wave from a transmitting antenna can be modeled as many ray tubes shooting from the location of the antenna [3] [4]. As shown in Fig. 2a, every ray tube is composed of four rays defined by the increments of θ and φ in new method, and all the significant radiation regions over a sphere centered at the antenna should be covered by the ray tubes. The transmitter modeled as a point source in an environment. In order to determine all possible rays that may leave the transmitter and arrive at the receiver, it is necessary to consider all possible angles of departure and arrival at the transmitter and receiver. Rays are launched from the transmitter at an elevation angle θ and azimuth angle φ relative to the standard engineering coordinate system. Antenna patterns are incorporated to include the effects of antenna beamwidth in both azimuth and elevation. The surface of surrounding sphere of source should be divided into several belts, each belt having a unique elevation angle θ and segmented into quadrilateral tubes with almost identical solid angle (Fig. 2a). The wave stems from diffracting edges is modeled as a belt of tubes similar to each belt of transmitter case, as demonstrated in Fig. 2b. This new method of diffraction modeling can be used to simulate inter-raypath diffractions in 3D SBR precisely based on cylindrical character of diffracted wave.

Each belt is constructed from the paired rays and each two-ray is shared between two adjacent tubes, where identified by a number identical to the number of tube in left side and assumed to that tube it belongs. In terms of numerical arrangement, the n^{th} two-ray would be shared by the $(n-1)^{th}$ and n^{th} tubes, except for n=0 which would be shared by last and first tubes of the considered belt of tubes, logically (Fig. 3). Therefore, for a belt with N tubes, N two-rays should be defined wherein a Boolean N-element array **T** assigns a Boolean tag for each tube, correspondingly. Each element of Boolean array, which

correspond a tube, is an aid to distinguish tracing possibility in each tracing step. In other words, tubes in this ray tracing method have no real interpretation and only are a binding concept of two adjacent two rays.

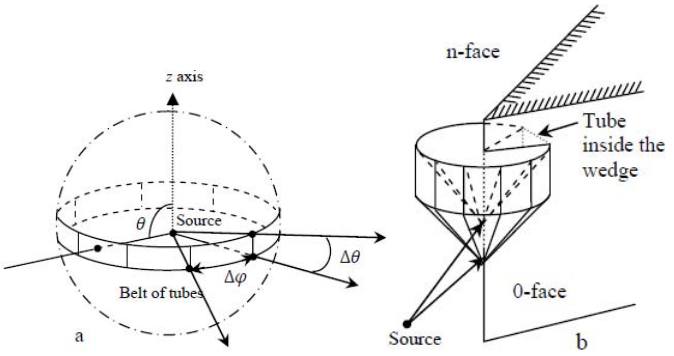

Figure 2. Configuration of tube belt a) ray tubes over a sphere centered at the antenna, and, b) ray tube stems from diffracting edge

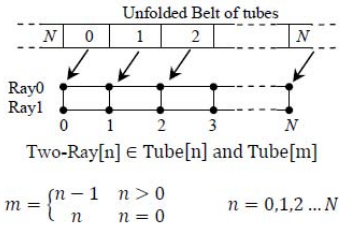

Figure 3. Tube belt architecture and **T** array

IV. NEW TRACING PROCEDURE

At the first stage all necessary belts should be created, based on shooting status. There are two different shooting status: rays originating from the transmitter source directly, or from at the diffracting wedge as a secondary belt source (Figure 1b). In case of rays originating from the source, a belt of tubes with True-valued elements in corresponding **T** array would be created at each unique elevation angle θ. In case of a two-ray obstructs a wedge, diffracted rays manipulated by a belt starting from the 0-face to the n-face with True-valued elements in corresponding **T** array, except for the tube inside the wedge. At the second stage, any admissible ray would be shot in order to find probable incidence point. An admissible ray is a ray that at least one of its two relevant tubes has True value in **T** array. All True-valued tubes, then, examined if received at receiving point(s). Third stage resets the Boolean value for each tube. First the field strength value of two-ray right side to the first tube is updated if they hit the same facet. Then, True value set for reflecting tube and False value set if otherwise (in case of diffraction or travelling without incidence). For a reflecting tube all its four rays have to collies same facet. Obviously, the rays of a tube do not have the same obstructing facet, or there are no obstructing facets at all, tube is identified as non-reflecting one. Aforementioned step can shed more light on that feature of method by which it can detect any discontinuing on the pass of coherent tubes (there are coherency because of two-ray sharing between tubes). Ray coherence means that similar rays are likely to intersect the same object in the environment. Thus, two rays, which have nearly the same origin and direction, are likely to trace out similar paths through the environment, hitting the same objects in nearly the same places. This is clearly related to connectedness and smoothness properties of the objects, and is therefore another manifestation of object coherence.

Finally, direction of propagation and field strength value of rays processed to enter this stage should be revised if distinguished necessary as following: a two-ray right side to the True-valued tube and a two-ray left side to the True-valued tube if the preceding tube is False-valued. An example for this approach is given in the following section. After above steps the changed **T** array will be considered as initial array to pass steps. Program operates these steps in a recursive and repetitive manner for each tube-belt emitted from a source or diffracting edge until a terminating criterion (threshold, maximum times of each mechanism or both) would meet.

V. A SIMPLE EXAMPLE

In this section a simple example environment assumed and the algorithm applied. As Fig. 4 displays, a belt segment of five true-valued tubes are shot to an environment contains two buildings and interception points are calculated. After that, for each tube, Boolean value associated with its array number at **T** array would be set based on the collision status of its ray pair and those of the next ray pair. As it could be understood, all four rays of tube n, (composed of n^{th} and $n+1^{th}$ pairs) has collided and their collision points are located on the same wall. So, the True value would be attributed to it. On the other hand, although, the four rays of $n+1^{th}$ tube, (composed of $n+1^{th}$ and $n+2^{th}$ pair) has collided with environment but their collision points are located on different walls and consequently it takes False value. Now, in order to update the field strength and direction of bounced rays, forth step goes as follow. Right pair of n^{th} tube ($n+1^{th}$ pair), $n+2^{th}$ tube ($n+3^{th}$ pair), $n+3^{th}$ tube ($n+4^{th}$ pair), $n+7^{th}$ tube ($n+8^{th}$ pair) would be updated. Based on the above idea left pair of True-valued tubes coming after a False-valued tube, should also be updated. Consequently, left pair of $n+2^{th}$ tube ($n+2^{th}$ pair), $n+7^{th}$ tube ($n+7^{th}$ pair) would also be updated. Hereafter, updated rays and **T** array are used for higher order bouncing, using mentioned procedure recursively. Relevant **T** array is displayed in Fig.4.

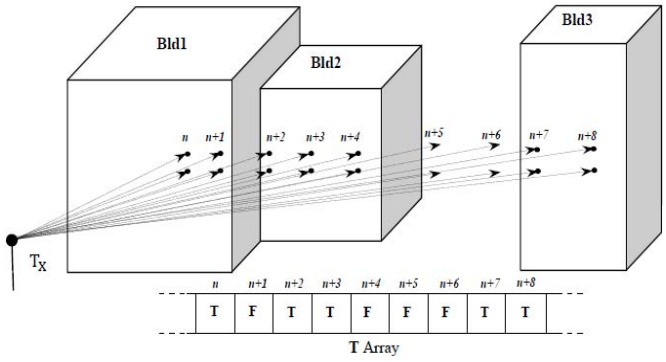

Figure 4. A simple representation of propagation environment

VI. Comparision of TRTT and CST Simulations

This section presents ray-tracing results for wave propagating in 3D structures, and compares the results with those obtained from the commercial electromagnetic simulation software CST MICROWAVE STUDIO®. The time-domain solver implemented in CST MWS is based on the finite integral time-domain method (FITD). FITD is the combination of finite integral technique (FIT) and perfect boundary approximation (PBA®) technique that outperforms other time domain numerical method, FDTD, by orders of magnitude not only in speed but also in accuracy. Therefore, the solutions determined by the CST are numerically exact, as long as the segmentation of the objects is small enough. Due to the limitations of the computer memory and CPU time, the FITD is usually applied for analyzing smaller objects in wavelengths. On the other hand, the ray-tracing method is a high-frequency approximation technique, which requires the dimensions of the objects be in the order of wavelengths or larger for accurate results, therefore, it is more suitable for modeling the indoor and outdoor wave propagation for wireless communications. However, by choosing structures with dimensions around a few wavelengths, CST can be used to examine the ray-tracing program. A 3D problem simulated using both the CST software and TRTT (Fig.5). Buildings of brick walls (ε_r =4.44, σ =0.001) and a typical ground (ε_r =15,σ =0.005) are assumed to apply. Ray tracing assume an infinite unit electric-line source (h_{Tx} = 3m) while CST attribute a finite small dimension in order to model the source. In ray tracing computations, in order to achieve high accuracy followings is done: setting the ray tube angle to be 0.1° and considering a combination of interactions equal to 20R-2D, where R and D indicates the number of reflections and diffractions which have been taken in account. Fig. 6 shows electric field distribution along OO' of Fig.5 at the frequency of 300MHz.

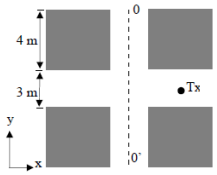

Figure 5. 2D environment used to calculate E field (height is 5 m).

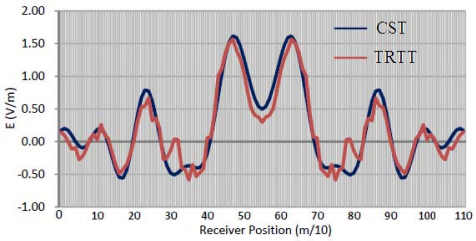

Figure 6. Comparison of E-field for TRTT and MoM at 300 MHz.

The size of the structures is just a few wavelengths and problem can be accurately solved by the MM. From the other side, their dimensions are also large enough for the ray-tracing method. However, due to not considering transmission through the walls and buildings, some discontinuities exist in the ray-tracing results. In addition, the locations and values of the peaks and valleys are slightly different between those two solutions. Nevertheless, the overall field variations obtained from those two methods is still quite similar. The good agreements between two results verify the ray-tracing program. It is noteworthy that the computation time of MM for such configuration with 13994640 meshes is 62646 sec which is almost 58 times greater than TRTT computation time (0:18').

VII. Comparision of TRTT Simulation and Field Measurements

In order to demonstrate the capability of the presented ray tracing techniques, a practical case study is investigated. It consists of 17 buildings, comprising 80 faces and edges, as illustrated in Fig. 7. The scenario represents the core of Ottawa, Canada, for which UTD-based results [8] and measurements [9] for the vertical polarization at 910MHz are available in the literature. Fig. 7 also depicts the transmitter (T) and receivers (dotted line) locations, with heights equal to 8.5 m and 3.65 m, respectively. More details about the geometrical and electrical features can be obtained in [8] and [9]. The TRTT algorithm was applied, considering 3-D trajectories from T_X to R with eight reflections and one diffraction, at most.

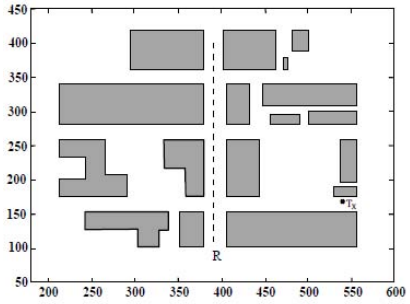

Figure 7. Plane view of the Ottawa city core. The transmitter is at T and receivers (R) are placed along Bank St. (dotted line)

For the urban environment of Fig. 7, 300 receivers where placed along the dotted line (Bank St.), with intervals of 1m. Fig. 8 illustrates path loss predictions along Bank St. (marked with a dotted line in Fig. 7). The UTD estimates were obtained with the help of the ray-tracing algorithm presented in [10]. The measured data was obtained from [9]. It can be seen the TRTT simulated results shown in Fig. 8 follow the trend of the measurements better than that of [10]. Most of the peaks and valleys of the measurements also coincide well with those of the simulations. The area calculation result depicted in Fig. 9.

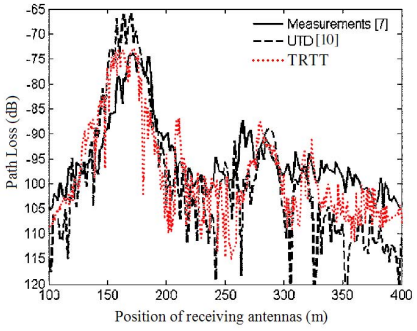

Figure 8. TRTT-predicted and measured path loss for Ottawa.

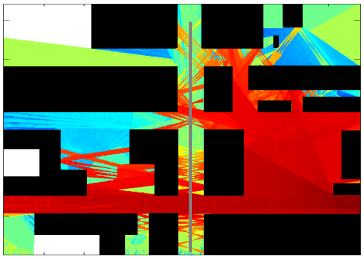

Figure 9. Area calculation result for the environment depicted in Fig. 7.

All the computation times have been measured on an Intel® Pentium® Mobile processor 2GHz, running Microsoft Windows XP Professional™ with 1GB of RAM. They correspond to the same configuration as above (with 8R- 1D). To evaluate TRTT performance, we have considered a naive version (four-ray tube configuration) of TRTT, which goes on tube-by-tube in contrast with belt-by-belt procedure of TRTT. Table I illustrate the computation of TRTT and conventional four-ray tube tracing method in seconds.

TABLE I. COMPUTATION TIME FOR DIFFERENT ENVIRONMENT DATA BASE

Environment	TRTT	4Ray Tube config.
Test Scenario, Figure 5	1082 sec	2189 sec
Core of Ottawa, Figure 7	620 sec	1251 sec

Consequently, the use of ray sharing idea saves 50% in the processing time. In conclusion, a significant reduction time factor is obtained without any loss of accuracy. It is notable that the computational time for first simple scenario is greater that second dense scenario because of settings of getting very high accurate results consist of tube resolution and number of interactions.

VIII. CONCLUSIONS

Predominance of lateral-tube tracing approach to the center-ray tracing approach proofed for the modeling of problem geometry and ray tracing, especially diffraction from wall edges, in section II, in the expense of allocating more rays per tube and spending more computational time. To benefit from the accurate solution of lateral-tube tracing approach, a new approach proposed here, called two-ray tube tracing (TRTT), in which the computation time of accurate four-ray tube tracer reduced in factor of 2 using ray tube coherency idea. In the TRTT method, shared ray pairs are intersected, evaluated, and updated once during tracing from source to the reception point. Use of TRTT method, eliminates needs of several costly tests required in center-ray tube tracing method and shrinks computation time of TRTT to comparable amount. TRTT solution for a simple environment a lossy ground has been compared with those determined from the MM. Good agreements have been obtained, even, more details observed. Then, the TRTT method has been applied to evaluate the fields at 910 MHz in the core of Ottawa for comparisons with the available measurements. The simulated solutions follow the trend of the measured results amazingly. Accurate results obtained by this ray-tracing method, proofs its capability in solution of outdoor wave propagation and calculation of wireless communication channel characteristics.

REFERENCES

[1] H. Ling, R. Chou, and S. Lee, "Shooting and bouncing rays: Calculating the RCS of an arbitrarily shaped cavity," IEEE Trans. Antennas Propagat., vol. 37, pp. 194–205, Feb. 1989.

[2] S. Y. Seidel and T. S. Rappaport, "Site-specific propagation prediction for wireless in-building personal communication system design," IEEETrans. Veh. Technol., vol. 43, pp. 879–891, Nov. 1994

[3] S. Chen and S. Jeng, "An SBR/image approach for radio wave propagation in indoor environments with metallic furniture," IEEE Trans. Antennas Propagat., vol. 45, pp. 98–106, Jan. 1997.

[4] C. Yang, B.Wu, and C. Ko, "A ray-tracing method for modeling indoor wave propagation and penetration," IEEE Trans. Antennas Propagat., vol. 46, pp. 907–919, June 1998.

[5] H. Suzuki and A. S. Mohan, "Ray tube tracing method for predicting indoor channel characteristic map," Electron. Lett., vol. 33, no. 17, pp. 1495–1496, 1997.

[6] G. Durgin, N. Patwari, and T. S. Rappaport, "Improved 3-D ray launching method for wireless propagation prediction," Electron. Lett., vol. 33, no. 16, pp. 1412–1413, 1997.

[7] Z. Yun, M. F. Iskander, and Z. Zhang, "Development of a new shooting-and-bouncing ray (SBR) tracing method that avoids ray double counting," in IEEE AP-S Int. Symp. Dig., vol. 1, pp. 464–467, Jul 2001.

[8] S. Y. Tan and H. S. Tan, "Propagation model for microcellular communications applied to path loss measurements in Ottawa City streets," IEEE Trans. Veh. Tech., vol. 44, no. 2, pp. 313–317, May 1995.

[9] J. H. Whitteker, "Measurements of path loss at 910 MHz for proposed microcell urban mobile systems," IEEE Trans. Veh. Technol., vol. 37, . no. 3, pp. 125–129, Aug. 1988.

[10] D. N. Schettino, F. J. S. Moreira, and C. G. Rego, "Efficient Ray Tracing for Radio Channel Characterization of Urban Scenarios," IEEE Trans. Magnetics, Vol. 43, No. 4, pp. 1305-1308, Apr. 2007.

[11] M. F. Cátedra, J. Pérez, F. Saez de Adana, and O. Gutiérrez, "Efficient ray-tracing technique for three-dimensional analyzes of propagation in mobile communications: Application to picocell and microcell scenarios," IEEE Antennas Propagat. Mag., vol. 40, pp. 15–28, Apr. 1998.